Curr Genet (2010) 56:87–100
DOI 10.1007/s00294-009-0282-6

RESEARCH ARTICLE

RAD59 and *RAD1* cooperate in translocation formation by single-strand annealing in *Saccharomyces cerevisiae*

Nicholas R. Pannunzio · Glenn M. Manthey · Adam M. Bailis

Received: 19 August 2009 / Revised: 24 November 2009 / Accepted: 25 November 2009 / Published online: 11 December 2009

Abstract Studies in the budding yeast, *Saccharomyces cerevisiae,* have demonstrated that a substantial fraction of double-strand break repair following acute radiation exposure involves homologous recombination between repetitive genomic elements. We have previously described an assay in *S. cerevisiae* that allows us to model how repair of multiple breaks leads to the formation of chromosomal translocations by single-strand annealing (SSA) and found that Rad59, a paralog of the single-stranded DNA annealing protein Rad52, is critically important in this process. We have constructed several *rad59* missense alleles to study its function more closely. Characterization of these mutants revealed proportional defects in both translocation formation and spontaneous direct-repeat recombination, which is also thought to occur by SSA. Combining the *rad59* missense alleles with a null allele of *RAD1*, which encodes a subunit of a nuclease required for the removal of non-homologous tails from annealed intermediates, substantially suppressed the low frequency of translocations observed in *rad1*-null single mutants. These data suggest that at least one role of Rad59 in translocation formation by SSA is supporting the machinery required for cleavage of non-homologous tails.

Communicated by M. Kupiec.

N. R. Pannunzio · G. M. Manthey · A. M. Bailis
Department of Molecular and Cellular Biology,
Beckman Research Institute of the City of Hope,
Duarte, CA 91010, USA

N. R. Pannunzio (✉)
The Irell and Manella Graduate School of Biological Sciences,
Beckman Research Institute of the City of Hope,
1500 E Duarte Road, Duarte, CA 91010, USA
e-mail: npannunzio@coh.org

Keywords Homologous recombination · DNA double-strand breaks · Ionizing radiation · Single-strand annealing · Translocations

Introduction

Living systems have evolved mechanisms to repair damaged genetic material following a variety of environmental insults, such as ionizing radiation. Modern civilization has increased the likelihood of human exposure to acute doses of radiation by either accidental causes (Lindholm and Edwards 2004) or as part of a therapeutic regimen (Muller et al. 2005). Among the various types of damage that can occur are DNA double-strand breaks (DSBs), which can be lethal if not repaired (Resnick and Martin 1976). Repair can either utilize a homologous template or proceed by homology-independent pathways. Homologous recombination (HR) can maintain chromosome stability by using the sister chromatid or homologous chromosome as a template for repair. However, many studies have demonstrated that HR between homologous sequences dispersed throughout the genome can readily generate genome rearrangements, such as translocations (Haber and Leung 1996; Fasullo et al. 1998; Richardson and Jasin 2000; Argueso et al. 2008; Pannunzio et al. 2008). Given the large number of repetitive elements scattered throughout the yeast and human genomes (Kim et al. 1998; Li et al. 2001), the potential for ectopic HR events is quite high. Indeed, when entire *Saccharomyces cerevisiae* genomes are mapped following a massive dose of ionizing radiation, the majority of chromosomal aberrations detected are the result of HR between repetitive elements and duplicate genes (Argueso et al. 2008). Furthermore, comparison of multiple human genomes suggests that the extensive copy number variation

present could be a product of recombination events among repetitive sequences, illustrating the capacity for the genomes of higher eukaryotes to undergo aberrant HR (Zhang et al. 2009), and underscoring the potential for non-conservative repair to lead to the genome instability that is a precursor to a number of human diseases (Strout et al. 1998; Meltzer et al. 2002).

Previously, we described an assay performed in diploid *S. cerevisiae* cells that allows us to model the genome rearrangement that occurs following acute exposure to ionizing radiation (Pannunzio et al. 2008). Through genetic and molecular analyses, we found that a significant fraction of the surviving cell population contained a novel translocation chromosome formed by single-strand annealing (SSA). The central HR gene, *RAD52* (Game and Mortimer 1974; Resnick and Martin 1976), and its paralog, *RAD59* (Bai and Symington 1996; Wu et al. 2006), were found to be critically important for generating these translocations. Interestingly, simultaneous loss of both *RAD52* and *RAD59* led to a synergistic decrease in the frequency of these events, consistent with distinct contributions to translocation formation. Furthermore, we found a genetic interaction between null alleles of *RAD59* and *RAD1*, which encodes a subunit of a single-stranded DNA endonuclease (Sung et al. 1993; Tomkinson et al. 1993), that indicated Rad59 is working together with Rad1–Rad10 in post-annealing steps, fitting with previous studies of Rad59 (Sugawara et al. 2000).

The role of Rad52 in HR has been characterized extensively. Its function in vivo has been examined by analyzing the responses of collections of *rad52* mutants using a variety of recombination assays (Mortensen et al. 2002; Cortes-Ledesma et al. 2004; Lettier et al. 2006; Feng et al. 2007). In vitro studies of the biochemical activity of Rad52 protein have described its ability to anneal complementary single-stranded DNA molecules (Mortensen et al. 1996) and to mediate strand invasion by Rad51 (Sung 1997). Structural studies have been pursued down to the atomic level as the crystal structure of the N-terminal domain of the human homolog has been described (Kagawa et al. 2002). While the functions of Rad59 have been explored both in vivo (Bai and Symington 1996; Jablonovich et al. 1999; Sugawara et al. 2000; Feng et al. 2007) and in vitro (Petukhova et al. 1999; Davis and Symington 2001; Wu et al. 2006) information on *RAD59* is at a relative deficit as, to date, no systematic studies of *rad59* missense alleles have been published. Since several lines of evidence point to Rad59 having a role in HR separate from Rad52, a deeper examination of Rad59 is warranted.

In this study, we further explore the role of *RAD59* in translocation formation by constructing and testing the effects of several missense mutant alleles of the gene. Using residues conserved between Rad52 and Rad59 as our guide, we have made several alanine substitution mutations. The *rad59* mutants displayed frequencies of translocation formation by SSA that varied from a level close to that of the null mutant to a level that was essentially wild type. We observed very similar patterns of spontaneous deletion formation by HR between non-tandem direct repeats that has also been proposed to occur by SSA (Lin et al. 1990). When these missense alleles were combined with a *rad1*-null allele, they suppressed its negative effect on translocation formation. These results are consistent with Rad59 interacting with Rad1–Rad10 in the canonical mechanism for SSA, but also suggest that loss of Rad59 may allow for an auxiliary mechanism for repair in the absence of Rad1. These results also indicate that the conserved structures to which the mutated residues contribute are important determinants of Rad59 function in SSA. Since the deletions and translocations generated by SSA can result in extensive loss of heterozygosity, SSA may contribute significantly to the tumorigenic effect of ionizing radiation exposure.

Materials and methods

Strains

Strains used in this study are listed in Table 1. All strains are isogenic to the W303 background unless otherwise indicated (Thomas and Rothstein 1989). Standard techniques for yeast growth and genetic manipulation were used (Sherman et al. 1986). Construction of the *rad52Δ*, *rad1Δ*, *msh2Δ*, and *rad59Δ* disruption alleles have been described previously (Schild 1983; Ronne and Rothstein 1988; Reenan and Kolodner 1992; Pannunzio et al. 2008). The *MATa::LEU2* allele was made by disrupting the *MAT* locus with the *MATa::LEU2* fragment from pJH124 (Ray et al. 1991). Translocation frequencies reported in Table 2 were measured in strains with both *MAT* loci disrupted by the *LEU2* marker to ensure that HO cleavage only occurs at the translocation substrates whereas the frequencies in Figs. 4 and 8 are from strains with both *MAT* loci intact. Note that use of intact or disrupted *MAT* loci had no significant effect on translocation frequencies measured in otherwise wild-type or *rad59Δ* mutant strains. An effect was only seen in *rad52Δ* mutants, where a higher translocation frequency is measured in *MATa::LEU2/MATa::LEU2* strains compared to *MATa/MATα* strains (Pannunzio, et al. 2008), presumably due to increased viability following HO induction in *MATa::LEU2/MATa::LEU2* strains. Therefore, for consistency, the results of all translocation assays reported in Table 2 were obtained from *MATa::LEU2/MATa::LEU2* homozygotes. All other constructs are described below.

Table 1 *S. cerevisiae* strains used in this study

Strain	Genotype	Source
ABM197	*MATa::LEU2/MATa::LEU2, his3-Δ200/his3-Δ3′-HOcs, leu2-3,112/leu2::HOcs-his3-Δ5′$_{(300)}$, trp1-1/trp1::GHOK*[a]	This study
ABX1711	*MATa/MATα, his3-Δ200/his3-Δ3′-HOcs, leu2-3, 112/leu2::HOcs-his3-Δ5′$_{(300)}$, URA3/ura3-1, trp1-1/trp1::GHOK*	Pannunzio et al. (2008)
ABX2184	*MATa/MATα, his3-Δ200/his3-Δ3′-HOcs, leu2-3, 112/leu2::HOcs-his3-Δ5′$_{(60)}$, URA3/ura3-1, trp1-1/trp1::GHOK*	Pannunzio et al. (2008)
ABM203	Same as ABM197 except *rad52::TRP1/rad52::TRP1*	This study
ABM208	Same as ABM197 except *rad59::LEU2/rad59::LEU2*	This study
ABX1698	Same as ABX1711 except *rad59::LEU2/rad59::LEU2*	Pannunzio et al. (2008)
ABX1689	Same as ABX2184 except *rad59::LEU2/rad59::LEU2*	Pannunzio et al. (2008)
ABX2368	Same as ABX1711 except *ADE2/ade2-1*, *rad59-Y92A/rad59-Y92A*	This study
ABX2369	Same as ABX2184 except *ADE2/ade2-1*, *rad59-Y92A/rad59-Y92A*	This study
ABX2758	Same as ABX1711 except *rad59-K166A/rad59-K166A*	This study
ABX2757	Same as ABX2184 except *rad59-K166A/rad59-K166A*	This study
ABX2303	Same as ABX1711 except *TRP1/trp1::GHOK*, *rad59-K174A/rad59-K174A*	This study
ABX2304	Same as ABX2184 except *TRP1/trp1::GHOK*, *rad59-K174A/rad59-K174A*	This study
ABX2725	Same as ABX1711 except *rad59-F180A/rad59-F180A*	This study
ABX2708	Same as ABX2184 except *rad59-F180A/rad59-F180A*	This study
ABX1771	Same as ABX1711 except *rad1::LEU2/rad1::LEU2*	Pannunzio et al. (2008)
ABX2093	Same as ABX1711 except *rad1::LEU2/rad1::LEU2, rad59::LEU2/rad59::LEU2*	Pannunzio et al. (2008)
ABX1660	Same as ABX1711 except *msh2::hisG::URA3::hisG/msh2::hisG::URA3::hisG*	Pannunzio et al. (2008)
ABX2264	Same as ABX1711 except *rad59::LEU2/rad59::LEU2, msh2::hisG::URA3::hisG/msh2::hisG::URA3::hisG*	This study
ABX2613	Same as ABX1711 except *rad1::LEU2/rad1::LEU2, rad59-Y92A/rad59-Y92A*	This study
ABX2831	Same as ABX1711 except *rad1::LEU2/rad1::LEU2, rad59-F180A/rad59-F180A*	This study
ABX2827	Same as ABX1711 except *rad1::LEU2/rad1::LEU2, rad59-K166A/rad59-K166A*	This study
ABX1244	Same as ABX2184 except *rad1::LEU2/rad1::LEU2*	Pannunzio et al. (2008)
ABX2095	Same as ABX2184 except *rad1::LEU2/rad1::LEU2, rad59::LEU2/rad59::LEU2*	This Study
ABM148	Same as ABX2184 except *msh2::hisG::URA3::hisG/msh2::hisG::URA3::hisG*	Pannunzio et al. (2008)
ABX2263	Same as ABX2184 except *rad59::LEU2/rad59::LEU2, msh2::hisG::URA3::hisG/ msh2::hisG::URA3::hisG,*	This Study
ABX2614	Same as ABX2184 except *rad1::LEU2/rad1::LEU2, rad59-Y92A/rad59-Y92A*	This Study
ABX2867	Same as ABX2184 except *rad1::LEU2/rad1::LEU2, rad59-F180A/rad59-F180A*	This Study
ABX2866	Same as ABX2184 except *rad1::LEU2/rad1::LEU2, rad59-K166A/rad59-K166A*	This Study
ABM130	Same as ABX1711 except *TRP1/trp1-1*	Pannunzio et al. (2008)
ABX1708	Same as ABX1711 except *TRP1/trp1-1, rad59::LEU2/rad59::LEU2*	Pannunzio et al. (2008)
ABX2844	Same as ABX1711 except *TRP1/trp1-1, rad59-K174A/rad59-K174A*	This study
ABX2845	Same as ABX1711 except *trp1-1/trp1-1, rad59-Y92A/rad59-Y92A*	This study
ABX2846	Same as ABX1711 except *trp1-1/trp1-1, rad59-K166A/rad59-K166A*	This study
ABX2847	Same as ABX1711 except *trp1-1/trp1-1, rad59-F180A/rad59-F180A*	This study
ABM216	*MATa::LEU2/MATa::LEU2, his3-Δ200/his3-Δ3′-HOcs$_{(MUT)}$, leu2-3, 112/leu2::HOcs-his3-Δ5′$_{(300)}$, trp1-1/trp1::GHOK*	This study
ABM227	Same as ABM216 except *rad52::TRP1/rad52::TRP1*	This study
ABM210	Same as ABM216 except *rad59::LEU2/rad59::LEU2*	This study
ABX2652	*MATa::LEU2/MATa::LEU2, his3-11, 15/HIS3-sam1ΔSalI, sam1ΔBglII-HOcs/sam1::LEU2, sam2::HIS3/sam2::HIS3, trp1-1/trp1::GHOK*	This study
ABM264	Same as ABX2652 except *rad52::TRP1/rad52::TRP1*	This study
ABM281	Same as ABX2652 except *rad59::LEU2/rad59::LEU2*	This study
ABX192-1A	*MATa his3::URA3::his3*	Maines et al. (1998)

Table 1 continued

Strain	Genotype	Source
ABX1236-3A	Same as ABX192-1A except *rad52::TRP1*	This study
ABX2427-2A	Same as ABX192-1A except *rad59::LEU2*	This study
ABX2437-2A	Same as ABX192-1A except *rad59-Y92A*	This study
ABX2743-3A	Same as ABX192-1A except *rad59-K166A*	This study
ABX2430-3C	Same as ABX192-1A except *rad59-K174A*	This study
ABX2711-1C	Same as ABX192-1A except *rad59-F180A*	This study
W961-5A	*MATa HIS3*	John McDonald
ABX917-46D	*MATα HIS3 ura3::KAN-MX*	This study
ABX552-2D	*MATα LEU2 rad52::TRP1*	This study
ABX512-37A	*MATa HIS3 rad59::LEU2*	This study
ABX2351-1D	*MATα HIS3 URA3 rad59-Y92A*	This study
ABX2745-13A	*MATα HIS3 rad59-K166A*	This study
ABX2279-2B	*MATa TRP1 rad59-K174A*	This study
ABX2705-15A	*MATa HIS3 rad59-F180A*	This study
ABX1612-12B	*MATα HIS3 RAD52-3xFLAG-KAN-MX*	Meyer and Bailis (2008)
ABX1713-38B	*MATα HIS3 RAD59-3xFLAG-KAN-MX*	This study
ABT650	*MATα HIS3 URA3 rad59-Y92A-3xFLAG-KAN-MX*	This study
ABT655	*MATa HIS3 rad59-K166A-3xFLAG-KAN-MX*	This study
ABT653	*MATα URA3 rad59-K174A-3xFLAG-KAN-MX*	This study
ABT654	*MATα HIS3 rad59-F180A-3xFLAG-KAN-MX*	This study

All strains are isogenic to the W303 background (*ade2-1, can1-100, his3-11, 15, leu2-3, 112, trp1-1, ura3-1*). Only differences from this genotype are noted

[a] *trp1::GHOK*, the galactose inducible HO endonuclease at the *TRP1* locus marked with *KAN-MX*

Table 2 Loss of *RAD59* affects translocation formation but not gene conversion

Relevant genotype	Two-break stimulated translocation frequency (10^{-3})[a]	One-break stimulated translocation frequency (10^{-7})[b]	Ectopic gene conversion frequency (10^{-4})[c]
Wild type	32.0 ± 15.0 (1.0)	78.0 ± 17.0 (1.0)	11.0 ± 5.0 (1.0)
rad52	3.2 ± 0.7 (10.0)	7.4 ± 1.1 (10.5)	0.0036 ± 0.0027 (3,055.6)
rad59	0.55 ± 0.08 (58.2)	52.0 ± 7.0 (1.5)	6.7 ± 4.5 (1.6)

[a] Diploid DSB-induced assay where HO endonuclease creates breaks at both the *his3-Δ3′* substrate on chromosome XV and the *his3-Δ5′* substrate on chromosome III. Substrates share 311 bp of sequence homology. Fold reduction from the corresponding wild-type number is indicated in parentheses. Strains: ABM197 (wild type), ABM203 (*rad52/rad52*), ABM208 (*rad59/rad59*)

[b] Diploid DSB-induced assay where HO endonuclease only creates a break at the *his3-Δ5′* substrate on chromosome III due to a mutation at the HO recognition sequence adjacent to the *his3-Δ3′* substrate (Pannunzio et al. 2008). Substrates share 311 bp of sequence homology. Strains: ABM216 (wild type), ABM227 (*rad52/rad52*), ABM210 (*rad59/rad59*)

[c] Diploid DSB-induced assay measuring recombination between mutant *sam1* alleles at the endogenous locus on one copy of chromosome XII and the *HIS3* locus on one copy of chromosome XV. Recombination is induced by the creation of a break at the *sam1* locus by HO endonuclease. Strains: ABX2652 (wild type), ABM264 (*rad52/rad52*), ABM281 (*rad59/rad59*)

Construction of *rad59* missense alleles

The *rad59-Y92A* mutant allele was constructed using a multi-step PCR method. First, primer-1 (5′-AAA CAT TCG GGg cTG ATG GTT GG-3′), which contains the T→G and A→C base substitutions indicated in lowercase that changes residue 92 from a tyrosine to an alanine, and primer-2 (5′-TTC ACC TCT CGA GGA CAA AG-3′) were used to create a 214 bp-product spanning nucleotides 263–477 of the *RAD59* coding sequence. Next, primer-3 (5′-AAG GGT TAC GTA GAG GAG AAG-3′) and primer-4 (5′-CAA CCA TCA gcC CCG AAT GTT TC-3′), which contains the same base substitutions as primer-1, were used to create a 333 bp-product spanning from

49 bp upstream to nucleotide 284 of the *RAD59* coding sequence. These two PCR products share 22 bp of overlapping sequence, with the base substitutions included in this region, and were used as templates in a third PCR reaction using alternative forms of primer-2 and primer-3 (primer-2-kpn and primer-3-eco) that were engineered to contain a *Kpn*I and *Eco*RI restriction sites, respectively. This final 526 bp-product was cloned into the polylinker of pBluescript II (Stratagene) that had been digested with *Eco*RI and *Kpn*I. This plasmid was designated pLAY581 and was sequenced (Laragen, Los Angeles, CA, USA) to verify the presence of the intended mutation. A PCR fragment containing the wild-type *RAD59* sequence from 387 bp upstream to 299 bp downstream of the coding sequence was cloned into the *Sma*I site of pBluescript II to create pLAY566. The *Hin*dIII/*Xba*I fragment from pLAY566, which contains the entire wild-type *RAD59* sequence was cloned into YIp356R (Myers et al. 1986), a yeast integration plasmid, to create pLAY567. The *Sna*BI/*Xho*I fragment of pLAY567 was replaced by the *Sna*BI/*Xho*I fragment of pLAY581 producing an integration plasmid containing the full length *rad59-Y92A* sequence. pLAY584 was linearized with *Bgl*II and transformed into ABX917-46D, which bears the *ura3::KAN-MX* allele to prevent the plasmid from targeting *URA3*. Transformants were selected for uracil prototrophy and genomic Southern blot analysis was performed to confirm integration of the plasmid. Pop-out events were selected by plating cells to medium containing 5-FOA (Boeke et al. 1984). The presence of the *rad59-Y92A* allele was confirmed by allele-specific PCR. Following confirmation of chromosomal insertion, the strain was backcrossed three times against W961-5A before being used in experiments.

A similar procedure was used to produce the three other missense alleles. The primers used to construct *rad59-K174A* were primer-5 (5′-GAT GCG TTA gcG AAG GCG TTA TTG-3′), primer-6 (5′-TAT ATA AGT ACG TGA GAT CTA TTT G-3′), primer-7 (5′-CCC CCC GAA TTC TTT GTC CTC GAG AGG TGA ATG TTA TAA CAG GTC GAA AAA AGA GGC TGT AGG CGA TGC GTT Agc GAA GGC G-3′), and primer-6-kpn. The primers used to construct *rad59-F180A* were primer-6, primer-8 (5′-CGC TTA TTG AGC gcT GAA AAA ATC-3′), primer-9 (5′-TTT GTC CTC GAG AGG TGA ATG-3′), primer-10 (5′-CGA CAT AGT AAT TAT TTG TAA TCT TAG TCT CAT AAT CGA GTA TGA TTT TTT CAg cGC TCA ATA ACG C-3′), primer-9-eco, and primer-6-kpn. The primers used to construct *rad59-K166A* were primer-6, primer-11 (5′-AGG TCG AAA gcA GAG GCT GTA GG-3′), primer-12 (5′-CCC CCC GAA TTC TTT GTC CTC GAG AGG TGA ATG TTA TAA CAG GTC GAA Agc AGA GGC TG-3′), and primer-6-kpn.

Construction of FLAG-tagged alleles of *RAD59*

Construction of the C-terminally tagged *RAD52-3xFLAG-KAN-MX* allele has been described (Meyer and Bailis 2008). C-terminally tagged versions of wild-type and mutant Rad59 were made by a similar method. A fusion construct was created by PCR using a forward primer (5′-TAA TAG CAA GCC GAC TTT TAT CAA ATT GGA GGA TGC TAA AGG CAC GCA TAT CAA AAG GGA ACA AAA GCT GGA G-3′) and reverse primer (5′-TTT ATC AAG CAA AAT AAA TTT GCT ACT TGT GCC CTT TTT CTT CTT TTT TTT TCT ATA GGG CGA ATT GGG T-3′) that each contain 50 bp of *RAD59* sequence. These were used to amplify the relevant portion of the p3FLAG-KanMX vector (Guldener et al. 1996). The PCR fragment was transformed into cells and G418 recombinants were tested for insertion of the epitope and marker sequences at the *RAD59* locus by Southern analysis and sequencing.

Determination of gene conversion frequency

The design and execution of the DSB-stimulated *SAM1* ectopic gene conversion assay in haploid strains were described previously (Bailis et al. 1995). The same or similar components have been utilized to examine DSB-stimulated ectopic gene conversion in diploids. The *sam1-ΔBgl II-HOcs* substrate lies at the *SAM1* locus on one copy of chromosome XII. The *sam1::LEU2* allele at the *SAM1* locus on the other copy of chromosome XII contains a complete deletion of the *SAM1*-coding sequence that has been replaced with a *LEU2* marker, preventing interaction with *sam1-ΔBglII-HOcs*. The *sam1-ΔSal I* allele was inserted into the *HIS3* locus on one copy of chromosome XV. The *sam1-ΔBgl II-HOcs* and *sam1-ΔSal I* substrates were inserted in opposite orientations with respect to their centromeres to prevent the isolation of reciprocal recombinants. The coding sequences of both copies of *SAM2* on chromosome IV have been replaced with *HIS3* markers to prevent interaction with the *sam1* substrates. The *sam1-ΔBglII-HOcs* substrate can be cut by HO endonuclease expressed from a galactose-inducible *HO* gene integrated into the *TRP1* locus on one copy of chromosome IV. Cutting *sam1-ΔBglII-HOcs* with HO endonuclease creates broken ends that share 279 bp and 1.4 kb of homology with the *sam1-ΔSal I* donor sequence.

All Sam$^-$ strains were maintained on YPD (2% dextrose, 2% bacto-peptone, 1% yeast extract) agar supplemented with 100 μg/ml *S*-adenosylmethionine (AdoMet) (Sigma-Aldrich, St. Louis, MO, USA). Assaying gene conversion was initiated by using single colonies to inoculate cultures of complete synthetic medium

containing 3% glycerol and 3% lactate as carbon sources and supplemented with 100 μg/ml AdoMet. Cultures were grown to saturation at 30°C before the addition galactose to 2% followed by a further 4-h incubation at 30°C. Dilutions of each galactose-induced culture were plated onto YPD agar supplemented with 100 μg/ml AdoMet and incubated at 30°C for 4–5 days to determine viability. Appropriate dilutions of galactose-induced cells were plated onto unsupplemented YPD agar to determine the number of AdoMet prototrophic recombinants. The number of AdoMet protrophic recombinants were divided by the number of viable cells to determine frequencies of ectopic gene conversion. The median ectopic gene conversion frequency was determined from a minimum of 10 trials and a 95% confidence interval was calculated using Microsoft® Excel.

Determination of translocation frequency

HO-stimulated translocation frequencies were performed as previously described (Pannunzio et al. 2008). Briefly, 1 ml cultures of synthetic complete (SC) or YP medium containing 3% glycerol and 3% lactate were inoculated with single colonies and incubated for 24 h at 30°C. Galactose was added to a final concentration of 2% to induce expression of the HO endonuclease. After 4 h of induction, appropriate dilutions of the cells were plated to YPD to assess viability, and medium lacking histidine to determine the numbers of recombinants. Translocation frequency was determined by dividing the number of histidine prototrophic colonies by the total number of viable cells. The median translocation frequency was determined from a minimum of 10 trials and a 95% confidence interval was calculated using Microsoft® Excel. Selected His^+ recombinants were subjected to genomic Southern blot and chromosome blot analysis to confirm the presence of the tXV:III translocation product as previously described (Pannunzio et al. 2008).

Determination of direct-repeat recombination frequency

The direct-repeat recombination (DRR) assay was performed as previously described (Maines et al. 1998). Briefly, at the *HIS3* locus of chromosome XV was inserted an intact *URA3* marker flanked by 3′- and 5′-truncated fragments of *HIS3* gene that share 223 bp of homology. Single colonies grown on synthetic medium lacking uracil were dispersed in 1 ml synthetic medium that lacks uracil and grown to saturation at 30°C. Dilutions of the culture were plated onto YPD to determine the number of viable cells or to medium lacking histidine to select for recombinants. Recombination frequency is calculated as the number of histidine prototrophs over the total number of viable cells. The median frequency was determined from a minimum of 10 trials and a 95% confidence interval was calculated using Microsoft® Excel.

Western blot analysis

Western blot analysis was performed using established methods (Sambrook and Russell 2001). One-hundred microliters of a mid-log YPD culture from each of the strains expressing a FLAG-tagged protein was used for western analysis. Cells were washed in dH_2O once and resuspended in 50 μl dH_2O. Ten microliters was then added to 2 μl 1 M Tris–HCl, 2 μl 500 mM Tris(2-carboxyethyl)phosphine hydrochloride (TCEP), and 14 μl 2× loading buffer (166 mM Tris–HCl, pH 8.0, 53 mM Tris-Base, 26.6% glycerol, 5.3% SDS, 0.007% bromophenol blue). Samples were boiled for 10 min and resolved on a NuPAGE 4–12% Bis–Tris gel with MES running buffer in an XCell SureLock Mini-Cell (Invitrogen, Carlsbad, CA, USA). Protein was then transferred to an Immobolin-P membrane (Millipore, Billerica, MA, USA) using a Mini Trans-Blot Electrophoretic Transfer Cell (Bio-Rad, Hercules, CA, USA). The membrane was blocked in 5% milk then probed with primary antibody, ANTI-FLAG M2 (Sigma-Aldrich) and beta-Actin (Abcam, Cambridge, MA, USA) overnight at 4°C. The following day, the membrane was probed with the secondary antibody, goat anti-mouse HRP (Thermo Scientific, Rockford, IL, USA). A Pierce SuperSignal West Femto Kit (Thermo Scientific) was used to produce a chemiluminescence signal, which was detected using a Fotodyne (Hartland, WI, USA) Luminary/FX workstation. The signals from four, independent blots were then quantitated using ImageQuant software.

Determination of γ-ray sensitivity

Single colonies of the indicated strain were used to inoculate 5 ml YPD cultures that where grown to saturation at 30°C. Cells were pelleted, washed once in an equal volume of dH_2O, pelleted again, and resuspended in an equal volume of dH_2O. Cell number was assessed by hemocytometer count prior to exposing the cells to a ^{137}Cs source, housed in a J.L. Shepard Mark I Irradiator (San Fernando, CA, USA), to administer the indicated dose. Finally, 500–10,000 cells, depending on the strain, were plated onto YPD, and incubated at 30°C for 3 days. Plating efficiency is reported as the number of colonies appearing on the YPD plates divided by the number of cells plated and that quotient multiplied by 100. The median plating efficiency ± a 95% confidence interval was calculated from at least six independent trials.

Results

Distinct roles for *RAD52* and *RAD59* in double-strand break repair

Previously, we described an assay that measures frequencies of recombination between *his3* alleles truncated at either their 3′ or 5′ ends located at the *HIS3* locus on one copy of chromosome XV or the *LEU2* locus on one copy of chromosome III in diploid cells (Fig. 1; Meyer and Bailis 2008; Pannunzio et al. 2008). DSBs are initiated adjacent to each of the truncated alleles that share either 60 or 311 bp of sequence homology, so as to mimic the approximate size of common repetitive elements. The selectable translocation product resulting from homologous repair can be present in up to 10% of surviving cells. The genetic requirements for translocation formation implicate SSA as the repair mechanism responsible for creation of the novel tXV:III chromosome.

Our prior genetic analysis revealed that both the major homologous recombination protein Rad52 and its paralog Rad59 are essential for efficient translocation formation (Pannunzio et al. 2008). Interestingly, if we compare the necessity of *RAD52* and *RAD59* in another DSB-induced repair assay that measures ectopic gene conversion in diploid cells, we find a stark contrast (Table 2). Loss of *RAD52* decreases the gene conversion frequency over 3,000-fold, while loss of *RAD59* has no significant effect. Also, the frequency that translocations are formed following the creation of single DSB adjacent to only one of the recombination substrates is reduced 10-fold in a *rad52Δ/rad52Δ* homozygote whereas there is no reduction in a *rad59Δ/rad59Δ* homozygote (Table 2). These results are consistent with the loss of *RAD52* having highly pleiotropic effects for HR, while it appears that the major role of *RAD59* is in DSB repair by SSA. This indicates that the study of *RAD59* would provide an opportunity to better understand the mechanics of SSA.

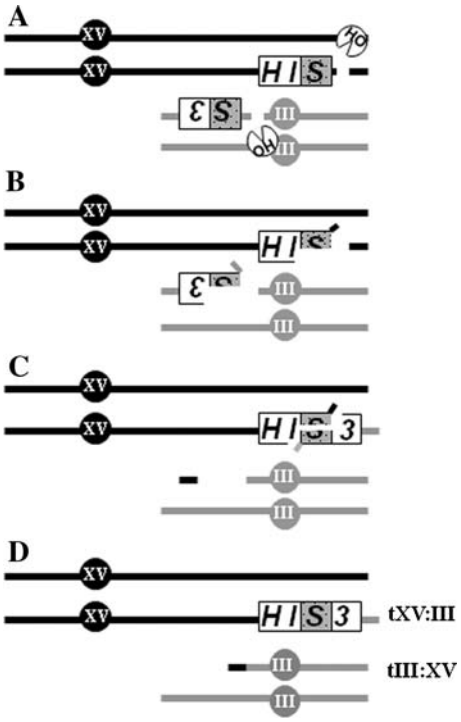

Fig. 1 Translocation assay. **a** A truncated *his3-Δ3′* allele is located on one copy of chromosome XV and a truncated *his3-Δ5′* allele is located on one copy of chromosome III. The *his3-Δ200* allele at the *HIS3* locus on the other copy of chromosome XV cannot contribute to the generation of an intact *HIS3* gene by HR. Upon addition of galactose, HO endonuclease is expressed and cutting occurs adjacent to each substrate. Note that in the "one-break" assay cutting only occurs adjacent to the *his3-Δ5′* substrate and in the "spontaneous" assay, HO endonuclease is not expressed. **b** Following DSB formation, end processing generates 3′ single-stranded DNA tails that can anneal, **c** via the 60 or 311 bp of overlapping sequence homology between the two substrates. **d** Terminal non-homology is then removed from the annealed intermediate allowing for ligation and creation of a tXV:III translocation chromosome that renders the cell prototrophic for histidine. The reciprocal tIII:XV translocation, which is generated by a mechanism that utilizes minimal shared homology between the chromosome fragments (G. Manthey and A. Bailis, unpublished data) is occasionally observed on chromosome and genomic Southern blots (Pannunzio et al. 2008)

Identification of *RAD59* missense alleles that decrease translocation formation by SSA

Missense alleles of *RAD52* have been found to lead to a variety of defects including reduced resistance to ionizing radiation, reduced frequencies of HR in several assays and reduced DNA binding by the Rad52 protein (Kagawa et al. 2002; Mortensen et al. 2002; Lloyd et al. 2005; Lettier et al. 2006; Feng et al. 2007). Many of these alleles are mutated at residues conserved between Rad52 and Rad59 (Feng et al. 2007). We hypothesized that alanine substitutions of some of these conserved residues in Rad59 might yield informative mutants. The Rad59 residues mutated for this study were Tyr92, Lys166, Lys174, and Phe180 (Fig. 2).

Since the phenotypes conferred by these mutations might be the result of altered stability of the Rad59 protein, we performed western blot analysis to assess the amounts of Rad59 relative to a β-actin control in wild-type and mutant cells (Fig. 3). Immunological detection of the wild-type and mutant gene products on western blots was accomplished by the construction of *RAD59* alleles at the native locus that append three copies of the FLAG epitope to the carboxy terminus of the protein. When the translocation assay was performed in strains containing FLAG-tagged versions of Rad52 and Rad59, a wild-type frequency was observed, indicating that the tag does not affect the function of the proteins (N. Pannunzio and A. Bailis, unpublished observations). The western analysis confirmed

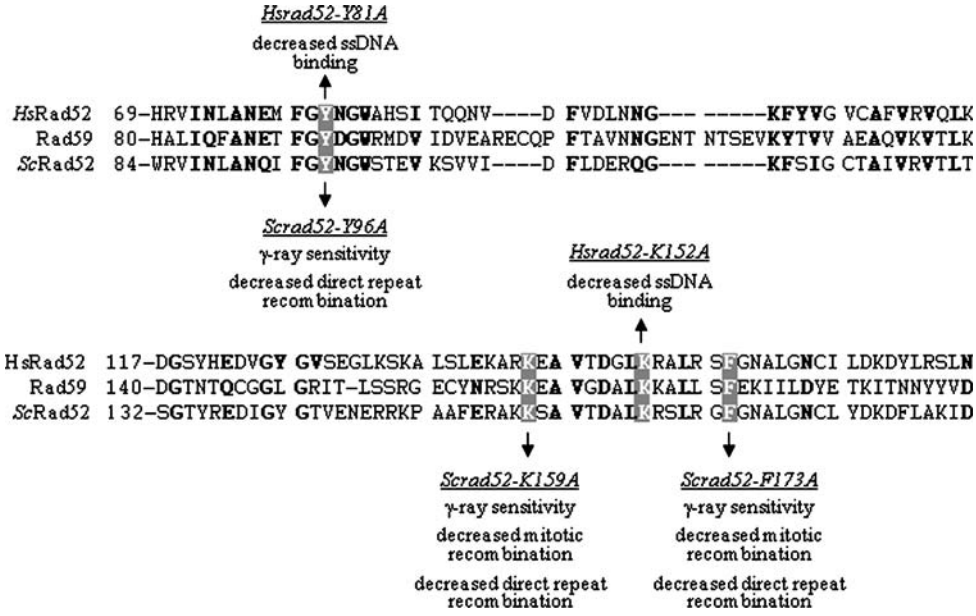

Fig. 2 Alignment of amino acid residues conserved between Rad59, *Sc*Rad52 and *Hs*Rad52. Portions of the Rad59, *Saccharomyces cerevisiae* Rad52 (*Sc*Rad52) and *Homo sapiens* Rad52 (*Hs*Rad52) amino acid sequences were aligned using the Multalin program. The Rad59 residues that were mutated to alanine in this study are highlighted with a *gray box*. In order, these are Tyr92, Lys166, Lys174, and Phe180. The in vitro or in vivo effects of these mutations in *Sc*Rad52 (Mortensen et al. 2002) or *Hs*Rad52 (Kagawa et al. 2002; Lloyd et al. 2005) are indicated

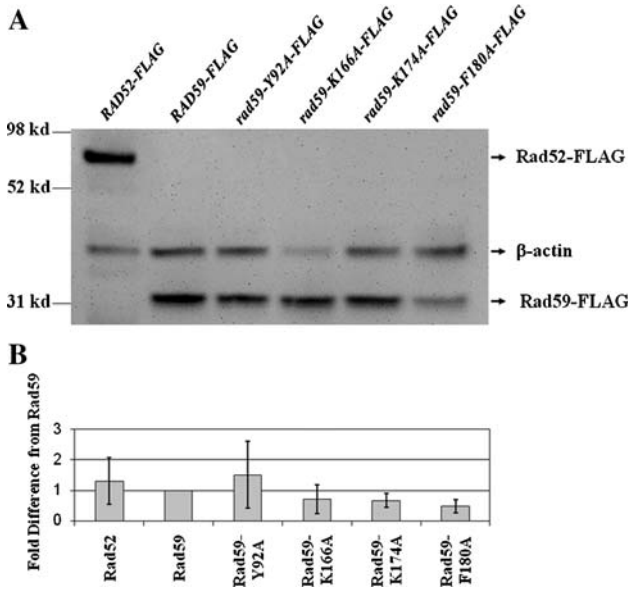

Fig. 3 Western blot analysis of the levels of Rad52 and Rad59 in wild type and *rad59* mutant cells. **a** Protein extracts were prepared from strains expressing FLAG-tagged versions of the indicated proteins. Anti-FLAG and anti-β-actin were used as the primary antibodies and an HRP conjugated goat anti-mouse was used for the secondary. **b** The graph displays the mean fold-difference from wild-type Rad59 from four independent determinations of Rad52 or Rad59 normalized to the level of β-actin in wild-type or *rad59* mutant cells

that the amount of Rad59 in the mutants does not differ greatly from the wild type (Fig. 3a, b). Of the four mutants, *rad59-F180A* displayed the lowest median normalized level of protein, 2.1-fold lower than wild type. These results indicated that the effects on the phenotypes of the *rad59* mutants that exceed 2- or 3-fold are unlikely to be attributable to changes in the steady-state levels of Rad59.

Previously, we found that the frequency of translocation formation in a *rad59Δ/rad59Δ* homozygote was reduced more than 50-fold with the 60 bp substrates and nearly 100-fold with the 311 bp substrates (Pannunzio et al. 2008). While none of the *rad59* missense mutants exhibited translocation frequencies that were as low as the null, the *rad59-K166A/rad59-K166A* and *rad59-F180A/rad59-F180A* homozygotes presented the most severe defects (Fig. 4). The *rad59-K166A/rad59-K166A* homozygote displayed 20- and 35-fold reduced translocation frequencies with the 60 and 311 bp substrates, respectively, while the *rad59-F180A/rad59-F180A* homozygote displayed 9- and 23-fold reduced frequencies. Interestingly, the *rad59-K174A/rad59-K174A* homozygote, which possesses a mutation at a conserved lysine that lies between the K166 and F180 residues, displayed no significant translocation defect suggesting that the conserved amino acids in this region do not contribute equally to the function of Rad59 in translocations. The *rad59-Y92A/rad59-Y92A* homozygote displayed translocation frequencies that were intermediate to the *rad59-F180A/rad59-F180A* and wild-type homozygotes, being reduced 3-fold with the 60 bp substrates and 5.5-fold with the 311 bp substrates. Together, these results indicate that the conserved amino acids of Rad59 do not contribute equally to its function in translocation formation by SSA.

The *RAD59* missense alleles similarly affect DRR

Spontaneous deletion formation through DRR is also proposed to occur by SSA (Schiestl et al. 1988; Schiestl and Prakash 1988). Therefore, we wanted to determine if the *rad59* mutant alleles exerted a similar effect on intrachromosomal DRR as they do on interchromosomal translocation

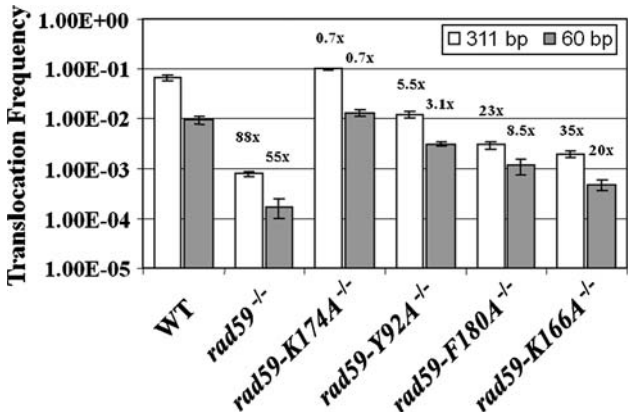

Fig. 4 The effect of *rad59* missense mutations on translocation formation by SSA. Translocation frequency using *his3* substrates with either 311 (*white bars*) or 60 bp (*gray bars*) of overlapping homology was measured in each of the indicated strains. Median frequencies and 95% confidence intervals were determined from a minimum of 10 independent trials. The fold-reduction from wild type is indicated above each bar. Strains: ABX1711 (*RAD59/RAD59*, 311 bp), ABX2184 (*RAD59/RAD59*, 60 bp), ABX1698 (*rad59Δ/rad59Δ*, 311 bp), ABX1689 (*rad59Δ/rad59Δ*, 60 bp), ABX2303 (*rad59-K174A/rad59-K174A*, 311 bp), ABX2304 (*rad59-K174A/rad59-K174A,* 60 bp), ABX2368 (*rad59-Y92A/rad59-Y92A*, 311 bp), ABX2369 (*rad59-Y92A/rad59-Y92A*, 60 bp), ABX2725 (*rad59-F180A/rad59-F180A*, 311 bp), ABX2708 (*rad59-F180A/rad59-F180A*, 60 bp), ABX2758 (*rad59-K166A/rad59-K166A*, 311 bp), ABX2757(*rad59-K166A/rad59-K166A*, 60 bp)

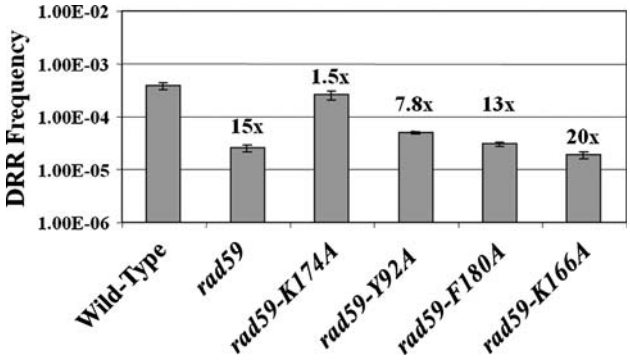

Fig. 5 The effect of *rad59* missense mutations on spontaneous DRR. The frequency of DRR between truncated *his3* alleles on chromosome XV that share 223 bp of overlapping sequence homology was measured in each of the indicated strains. Median frequencies and 95% confidence intervals were determined from a minimum of 10 independent trials. Strains: ABX192-1A (*RAD59*), ABX2427-2A (*rad59Δ*), ABX2430-3C (*rad59-K174A*), ABX2437-2A (*rad59-Y92A*), ABX2711-1C (*rad59-F180A*), ABX2745-13A (*rad59-K166A*)

formation. DRR was measured as deletions that occur on chromosome XV between 3′ and 5′ truncated copies of the *his3* gene that share 223 bp of sequence homology leading to histidine prototrophy (Maines et al. 1998). DRR was reduced 15.2-fold in the *rad59Δ* mutant (Fig. 5), demonstrating the importance of Rad59 in this repair process. For the *rad59* missense alleles, the trends observed were very similar to those noted for translocations. The *rad59-F180A* and *rad59-K166A* mutants were the most defective at 12.7- and 20-fold down, respectively, which are not significantly different from the DRR frequency in the *rad59Δ* null mutant. While the *rad59-K174A* mutant displayed no DRR defect, the *rad59-Y92A* mutant displayed an 8-fold reduction that, like the frequency of translocation formation in the *rad59-Y92A/rad59-Y92A* homozygote was intermediate to the frequency in the wild-type and the null mutant. The results of the translocation and deletion assays with the *rad59* mutants suggest that Rad59 exerts similar effects in both translocation and deletion formation by SSA.

RAD59 missense alleles have little effect on spontaneous translocation formation or radiation sensitivity

The tXV:III translocation chromosome can form spontaneously, albeit at the extremely low rate of 6×10^{-9} events/cell/generation in wild-type cells (Fig. 6; Pannunzio et al. 2008). The rarity of spontaneous translocations makes it difficult to determine a specific mechanism for their formation, but our prior chromosome blot analysis suggests a conservative mode of repair, in contrast to non-conservative SSA that occurs following creation of two DSBs. Interestingly, a *rad59Δ* mutant displays a slight, but significant, 2-fold increase in spontaneous translocation (Pannunzio et al. 2008; Fig. 6), suggesting that complete loss of *RAD59* can lead to a hyper-recombinogenic phenotype. Each of the *rad59* missense alleles was tested for its effect on spontaneous translocation formation, to determine if they caused hyper-recombination. None of the *rad59* missense mutants displayed rates of spontaneous translocation formation equivalent to that measured for *rad59Δ*. Of the four alleles, only *rad59-K166A* led to a translocation rate significantly different from wild type, being intermediate to wild type and the null with a 1.5-fold increase. These results confirm that Rad59 has little effect on spontaneous translocation formation.

Sensitivity to ionizing radiation is a hallmark of HR mutants since exposure leads to DSBs that, in yeast require repair by HR for a cell to survive (Game and Mortimer 1974; Resnick and Martin 1976). Loss of *RAD52* leads to severe radiation sensitivity while cells lacking *RAD59* have a much more subtle decrease in viability (Bai et al. 1999; Feng et al. 2007). Viability in a *rad52Δ* mutant decreases markedly even in response to relatively low doses of radiation, while a *rad59Δ* mutant exhibits wild-type levels of radiation sensitivity up to the 40 krad dose (Fig. 7). Each of the *rad59* mutant alleles was exposed to increasing doses of gamma radiation to test their sensitivity. The *rad59-F180A* mutant displayed a sensitivity that was similar to that of the *rad59Δ* strain, and was, in fact, slightly more sensitive than the null at the 40 krad dose. *rad59-K174A* again presented as wild type, but, interestingly, *rad59-Y92A* and *rad59-K166A*

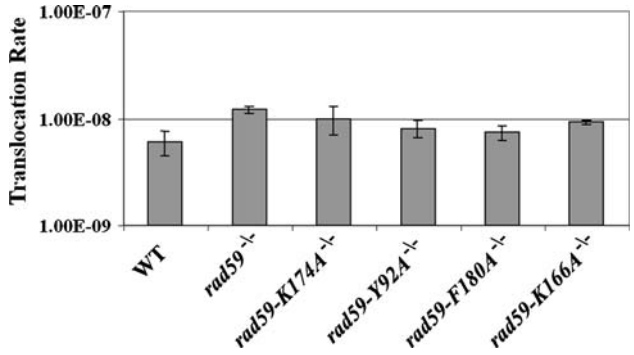

Fig. 6 The effect of *rad59* missense mutations on spontaneous translocation rate. The spontaneous translocation rate using *his3* substrates with 311 bp of overlapping homology was measured in each of the indicated strains. Rates were determined by the method of the median (Lea and Coulson 1949). Median rate and 95% confidence intervals were determined from a minimum of 10 independent trials. Strains: ABM130 (*RAD59/RAD59*), ABX1708 (*rad59Δ/rad59Δ*), ABX2844 (*rad59-K174A/rad59-K174A*), ABX2845 (*rad59-Y92A/rad59-Y92A*), ABX2846 (*rad59-K166A/rad59-K166A*), ABX2847 (*rad59-F180A/rad59-F180A*)

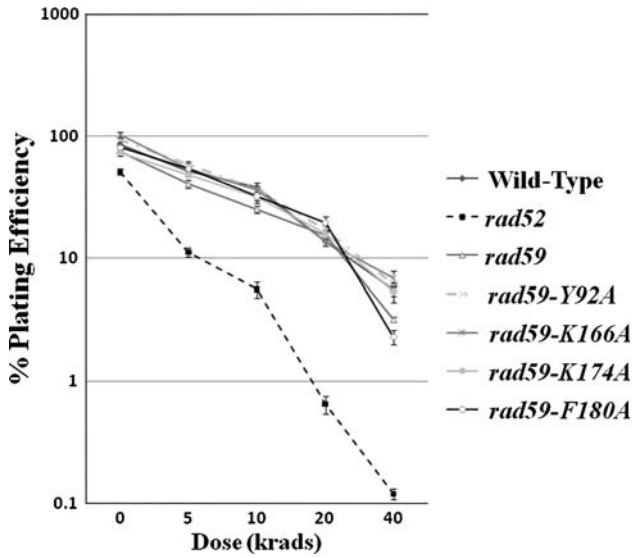

Fig. 7 Gamma-ray sensitivity of *rad59* missense mutants. Indicated strains were exposed to increasing does of ionizing radiation. Mean plating efficiencies were determined from a minimum of six independent trials. Strains: W961-5A (wild type), ABX552-2A (*rad52Δ*), ABX512-37A (*rad59Δ*), ABX2279-2B (*rad59-K174A*), ABX2351-1D (*rad59-Y92A*), ABX2705-15A (*rad59-F180A*), ABX2745-13A (*rad59-K166A*)

also show the same sensitivity as wild-type cells even though each was defective for both deletion and translocation formation by SSA.

The *rad59* missense alleles display distinct effects on translocation formation by SSA in the presence and absence of *RAD1*

The final steps of SSA require the removal of non-homologous ssDNA tails from annealed intermediates prior to ligation.

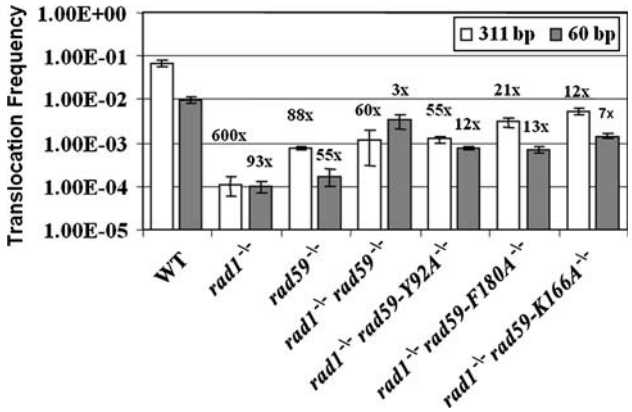

Fig. 8 *RAD1* epistasis analysis with *RAD59* missense mutants. Translocation frequency using *his3* substrates sharing either 60 or 311 bp of overlapping homology was measured in each of the indicated strains following the creation of DSBs. Fold change from wild type is indicated above each bar on the graph. Strains: ABX1711 (wild type, 311 bp), ABX2184 (wild type, 60 bp), ABX1771 (*rad1Δ/rad1Δ*, 311 bp), ABX1244 (*rad1Δ/rad1Δ*, 60 bp), ABX1698 (*rad59Δ/rad59Δ*, 311 bp), ABX1689 (*rad59Δ/rad59Δ*, 60 bp), ABX2093 (*rad1Δ/rad1Δ, rad59Δ/rad59Δ*, 311 bp), ABX2095 (*rad1Δ/rad1Δ, rad59Δ/rad59Δ*, 60 bp), ABX2613 (*rad1Δ/radΔ, rad59-Y92A/rad59-Y92A*, 311 bp), ABX2614 (*rad1Δ/radΔ, rad59-Y92A/rad59-Y92A*, 60 bp), ABX2831 (*rad1Δ/rad1Δ, rad59-F180A/rad59-F180A*, 311 bp), ABX2867 (*rad1Δ/rad1Δ, rad59-F180A/rad59-F180A*, 60 bp), ABX2827 (*rad1Δ/rad1Δ, rad59-K166A/rad59-K166A*, 311 bp), ABX2866 (*rad1Δ/rad1Δ, rad59-K166A/rad59-K166A*, 60 bp)

The products of the *RAD1* and *RAD10* genes form a nuclease (Sung et al. 1993; Tomkinson et al. 1993) that is required to remove these tails (Fishman-Lobell and Haber 1992). It has also been demonstrated that the central mismatch repair factor, Msh2, functioning in a heterodimer with Msh3, participates with Rad1–Rad10 in tail removal (Reenan and Kolodner 1992; Saparbaev et al. 1996; Lyndaker and Alani 2009). Previously, we found that loss of either *RAD1* or *MSH2* substantially reduced translocation formation (Pannunzio et al. 2008). Recent work from our lab has shown that simultaneous loss of both *RAD1* and *MSH2* suppresses the effects of losing either one individually and that *msh2* missense alleles confer differential abilities to suppress the effects of losing *RAD1* (Manthey et al. 2009). This is strikingly reminiscent of our previous epistasis analysis with the *rad1Δ* and *rad59Δ* alleles, which revealed that the loss of *RAD59* suppressed the reduced frequency of translocation formation conferred by the loss of *RAD1* (Fig. 8; Pannunzio et al. 2008). Given these similarities, translocation frequencies were measured in *msh2Δ/msh2Δ rad59Δ/rad59Δ* double homozygotes, and were found not to be statistically different from those observed in the *msh2Δ/msh2Δ* and *rad59Δ/rad59Δ* single homozygotes, demonstrating that *msh2Δ* and *rad59Δ* were completely epistatic to one another (Fig. 9). This suggests that Msh2 and Rad59 work together during translocation

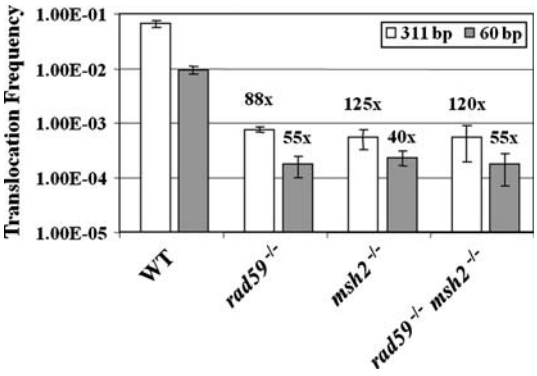

Fig. 9 *MSH2* and *RAD59* epistasis analysis. Translocation frequency using *his3* substrates sharing either 60 or 311 bp of overlapping homology was measured in each of the indicated strains following the creation of DSBs. Fold change from wild type is indicated *above each bar* on the graph. Strains: ABX1711 (wild type, 311 bp), ABX2184 (wild type, 60 bp), ABX1698 (*rad59Δ/rad59Δ*, 311 bp), ABX1689 (*rad59Δ/rad59Δ*, 60 bp), ABX1660 (*msh2Δ/msh2Δ*, 311 bp), ABM148 (*msh2Δ/msh2Δ*, 60 bp), ABX2264 (*msh2Δ/msh2Δ, rad59Δ/rad59Δ*, 311 bp), ABX2263 (*msh2Δ/msh2Δ, rad59Δ/rad59Δ*, 60 bp)

formation. Observing the epistatic relationship between *msh2Δ* and *rad59Δ*, and their similar effects when combined with the *rad1Δ* allele (Pannunzio et al. 2008; Manthey et al. 2009), led us to examine if, like several of the *msh2* alleles, the *rad59* missense alleles that affect SSA were capable of suppressing the translocation defect conferred by *rad1Δ*.

When the 311 bp substrates were used, the *rad59* missense alleles displayed variable capacities to suppress the effect of the *rad1Δ* allele (Fig. 8). The *rad59-Y92A* allele suppressed least, raising translocation levels in the *rad1Δ/rad1Δ rad59-Y92A/rad59-Y92A* double homozygote approximately 10-fold from that observed in the *rad1Δ/rad1Δ* homozygote, which is very similar to the level observed in the *rad1Δ/rad1Δ rad59Δ/rad59Δ* double homozygote. The *rad59-K166A* allele suppressed most, with translocation frequencies increased 50-fold in the *rad1Δ/rad1Δ rad59-K166A/rad59-K166A* double homozygote. Shortening the amount of homology available for recombination to 60 bp, had the effect of nearly erasing the differences in the abilities of the *rad59* missense alleles to suppress the effect of *rad1Δ*, as all three *rad1Δ/rad1Δ rad59/rad59* double homozygotes displayed translocation frequencies that were between 7- and 13-fold higher than that observed in the *rad1Δ/rad1Δ* homozygote. Notably, the translocation frequencies for all three of these double homozygotes were significantly below that of the *rad1Δ/rad1Δ rad59Δ/rad59Δ* double homozygote, indicating that with the short substrates, none of the *rad59* missense alleles were capable of suppressing the effect of losing *RAD1* as well as the *rad59Δ* null allele.

Discussion

Since its discovery, *RAD59* has been implicated in various types of intrachromosomal mitotic recombination events involving inverted or direct repeats while exhibiting limited effects on heteroallelic recombination (Bai and Symington 1996; Jablonovich et al. 1999; Sugawara et al. 2000; Feng et al. 2007). This implicates Rad59 as a major component of SSA, but dispensable for other types of HR. Our current results confirm these findings, as Rad59 was found to be essential for efficient inter- and intrachromosomal SSA (Figs. 4, 5), but to contribute little to other types of events (Table 2; Figs. 6, 7). The relevance of SSA to eukaryotic genome stability is clearly implied when one considers that translocation formation by recombination between repetitive elements is a major consequence of acute radiation exposure, which results in the creation of hundreds of DSBs per genome (Argueso et al. 2008), and that these processes are likely to be recapitulated in higher eukaryotes (Weinstock et al. 2006). Therefore, developing an understanding of the role of Rad59 in yeast SSA may provide greater insight into how genome stability is controlled in higher systems.

This study presents the characterization of four novel alleles of *RAD59*, three of which were found to lead to partial defects in translocation formation by SSA. These alleles bear mutations that alter amino acids conserved between Rad59 and Rad52. Information regarding the roles played by these amino acids in the function of Rad52, both in vivo and in vitro, suggests ways in which changing the analogous amino acids affect the function of Rad59. The crystal structure of the first 212 amino acids of human Rad52 reveals a monomer with a putative DNA-binding groove and a protrusion consisting of a *β–β–β–α*-fold. Following assembly into an undecamer complex, the *β–β–β–α* structure forms a round "stem" base and the binding groove creates a "domed-cap" with a positively charged channel running along the upper surface to accommodate DNA (Kagawa et al. 2002). All of the *rad59* mutants created in this study fall within the region that creates the *β–β–β–α* motif, which is the most highly conserved region between Rad59 and both yeast and human Rad52.

Tyr92 of Rad59 lies at the very beginning of the *β–β–β–α* motif. In *Hs*Rad52, the analogous Tyr81 protrudes from the monomer and fits into a hydrophobic pocket created on the neighboring monomer (Kagawa et al. 2002), indicating that this residue is important for quaternary structure. Therefore, the phenotype of the *rad59-Y92A* mutant may be due to a defect in its ability to associate with other Rad59 monomers, Rad52, or perhaps other SSA factors. Experiments performed in vitro with purified *Hs*Rad52 demonstrate that mutation of Tyr81 inhibits oligomerization of the C-terminally truncated (1–212) protein, but not the full-length

*Hs*Rad52 (Lloyd et al. 2005). This suggests that Tyr92 of Rad59, which is of similar dimensions as the C-terminally truncated *Hs*Rad52, may play a more important role in protein–protein interactions than in full length yeast and human Rad52, and may explain why we observed a somewhat more severe recombination defect conferred by the *rad59-Y92A* allele than that conferred by the analogous yeast *rad52-Y96A* allele (Mortensen et al. 2002; Lettier et al. 2006).

Mutation of the Lys166 and Phe180 residues of Rad59 resulted in the largest effects in our analysis, and both of these residues lie in the α-helix of the putative *β*–*β*–*β*–α motif. While the impact of the analogous mutations in the C-terminally truncated *Hs*Rad52 has not been reported, mutation of Lys152, which is also present in this helix, displays a clear defect in DNA binding (Kagawa et al. 2002; Lloyd et al. 2005), indicating that residues within the corresponding Rad59 helix, especially the positively charged Lys166, may be directly involved in physically contacting the DNA. Interestingly, mutation of Lys174 of Rad59 and Lys167 of *Sc*Rad52, which correspond to Lys152 of *Hs*Rad52, have not been observed to result in any effect on recombination (Figs. 4, 5; Mortensen et al. 2002). These results suggest that either this lysine is not involved in DNA binding by the yeast proteins or that DNA binding within this region of the yeast Rad52 and Rad59 proteins is not essential for recombination in vivo. Alternatively, slight variations in the amino acid sequence between Rad52 and Rad59 could result in this residue being on a turn of the α helix that does not allow for interaction. While these data make it difficult to predict which biochemical function of Rad59 may be disrupted by the *rad59-K166A* and *rad59-F180A* mutations, it is important to note that the analogous mutations in the yeast *RAD52* gene, *rad52-K159A* and *rad52-F173A*, confer quite significant recombination defects (Mortensen et al. 2002), suggesting that these conserved residues are important for the proper function of both proteins in HR. The relatively minor effects of these mutations on the steady state levels of Rad59 (Fig. 3) suggest that their effects on recombination are more likely due to defects in a conserved biochemical function than reduced levels of protein.

The Rad1–Rad10 nuclease is required to remove non-homologous DNA tails from annealed intermediates in the penultimate step of SSA (Fishman-Lobell and Haber 1992). While Rad59 demonstrates the ability to anneal complementary DNA (Petukhova et al. 1999), it has also been suggested that it participates in non-homologous tail removal (Sugawara et al. 2000; Pannunzio et al. 2008; Lyndaker and Alani 2009). Previously, we had shown that simultaneous loss of Rad1 and Rad59 resulted in levels of translocation formation by SSA that could substantially exceed those observed when either one alone was removed, suggesting that both suppress an alternative mechanism for removal of the non-homologous tails (Fig. 8; Pannunzio et al. 2008). This was distinct from results measured in *rad52Δ/rad52Δ rad1Δ/rad1Δ* double homozygotes, where translocation frequency remained at the level observed in the *rad1Δ/rad1Δ* single homozygotes, indicating that suppression of the translocation defect conferred by *rad1Δ* was specific to the *rad59Δ* allele (Pannunzio et al. 2008). Therefore, by examining the epistasis relationships between the *rad59* missense alleles and *rad1Δ*, we were able to further reveal a function of Rad59 that is distinct from that of Rad52.

Intriguingly, the *rad59* missense alleles had reciprocal effects on translocation formation by SSA in the presence and absence of *RAD1*, which is revealed most clearly by comparing the effects of the *rad59-Y92A* and *rad59-K166A* alleles (Figs. 4, 8). When *RAD1* is present, the *rad59-Y92A* allele results in a translocation frequency that is substantially higher than the frequency measured when it is absent, while, conversely, *rad59-K166A* confers considerably larger decreases in the presence of *RAD1* than when it is absent. The differential ability of these alleles to suppress the defect exhibited in a *rad1Δ/rad1Δ* homozygote demonstrates a clear genetic interaction between *RAD1* and *RAD59* and suggests that Rad59 executes a function in support of Rad1–Rad10-mediated cleavage of non-homologous tails, perhaps in facilitating the binding of Msh2–Msh3 (Sugawara et al. 2000; Lyndaker and Alani 2009; Manthey et al. 2009). Examination of the relationship between *msh2Δ* and *rad59Δ* indicates that they are epistatic to one another, with respect to translocation formation by SSA (Fig. 9), which suggests that Msh2–Msh3 and Rad59 work together in this process. Furthermore, our group recently found that the loss of *MSH2* suppresses the effect of losing *RAD1* on translocation formation in much the same way as the loss of *RAD59* (Manthey et al. 2009). This reinforces the notion that Rad59 and Msh2–Msh3 function together in supporting non-homologous tail cleavage by Rad1–Rad10.

With the construction of the *rad59* missense alleles described in this manuscript, we have acquired a better set of tools for dissecting how Rad59 supports SSA and determines the fate of broken chromosomes. The fact that the loss of *RAD59* only minimally affects the viability of the cells following acute radiation exposure (Fig. 7), but clearly changes the pattern of repair following the generation of multiple DSBs (Fig. 4) suggests that if a human ortholog can be identified, attenuating its expression in patients undergoing radiation therapy might be of clinical utility. Cell killing, and therefore efficacy of treatment, should be unaffected, but loss of heterozygosity events due to SSA-driven genome rearrangements should be reduced, perhaps minimizing the incidence of secondary cancers.

Acknowledgments The authors would like to thank S. Masri for her technical advice on western blot analysis and for useful commentary on the manuscript. This work was supported by funds from the National Institutes of Health (GM057484 to A. M. B.), the American Heart Association (AHA0615054Y to N. R. P.), the Department of Defense/Department of the Interior (1435-04-06-GT-63257 to G. M. M.), and the Beckman Research Institute of the City of Hope. The views and conclusions contained in this document are those of the authors and should not be interpreted as necessarily representing the official policies, either expressed or implied, of the U.S. Government.

References

Argueso JL, Westmoreland J, Mieczkowski PA, Gawel M, Petes TD, Resnick MA (2008) Double-strand breaks associated with repetitive DNA can reshape the genome. Proc Natl Acad Sci USA 105:11845–11850

Bai Y, Symington LS (1996) A Rad52 homolog is required for RAD51-independent mitotic recombination in *Saccharomyces cerevisiae*. Genes Dev 10:2025–2037

Bai Y, Davis AP, Symington LS (1999) A novel allele of RAD52 that causes severe DNA repair and recombination deficiencies only in the absence of RAD51 or RAD59. Genetics 153:1117–1130

Bailis AM, Maines S, Negritto MT (1995) The essential helicase gene RAD3 suppresses short-sequence recombination in *Saccharomyces cerevisiae*. Mol Cell Biol 15:3998–4008

Boeke JD, LaCroute F, Fink GR (1984) A positive selection for mutants lacking orotidine-5′-phosphate decarboxylase activity in yeast: 5-fluoro-orotic acid resistance. Mol Gen Genet 197:345–346

Cortes-Ledesma F, Malagon F, Aguilera A (2004) A novel yeast mutation, rad52–L89F, causes a specific defect in Rad51-independent recombination that correlates with a reduced ability of Rad52–L89F to interact with Rad59. Genetics 168:553–557

Davis AP, Symington LS (2001) The yeast recombinational repair protein Rad59 interacts with Rad52 and stimulates single-strand annealing. Genetics 159:515–525

Fasullo M, Bennett T, AhChing P, Koudelik J (1998) The *Saccharomyces cerevisiae* RAD9 checkpoint reduces the DNA damage-associated stimulation of directed translocations. Mol Cell Biol 18:1190–1200

Feng Q et al (2007) Rad52 and Rad59 exhibit both overlapping and distinct functions. DNA Repair (Amst) 6:27–37

Fishman-Lobell J, Haber JE (1992) Removal of nonhomologous DNA ends in double-strand break recombination: the role of the yeast ultraviolet repair gene RAD1. Science 258:480–484

Game JC, Mortimer RK (1974) A genetic study of X-ray sensitive mutants in yeast. Mutat Res 24:281–292

Guldener U, Heck S, Fielder T, Beinhauer J, Hegemann JH (1996) A new efficient gene disruption cassette for repeated use in budding yeast. Nucleic Acids Res 24:2519–2524

Haber JE, Leung WY (1996) Lack of chromosome territoriality in yeast: promiscuous rejoining of broken chromosome ends. Proc Natl Acad Sci USA 93:13949–13954

Jablonovich Z, Liefshitz B, Steinlauf R, Kupiec M (1999) Characterization of the role played by the RAD59 gene of *Saccharomyces cerevisiae* in ectopic recombination. Curr Genet 36:13–20

Kagawa W et al (2002) Crystal structure of the homologous-pairing domain from the human Rad52 recombinase in the undecameric form. Mol Cell 10:359–371

Kim JM, Vanguri S, Boeke JD, Gabriel A, Voytas DF (1998) Transposable elements and genome organization: a comprehensive survey of retrotransposons revealed by the complete *Saccharomyces cerevisiae* genome sequence. Genome Res 8:464–478

Lea DE, Coulson CA (1949) The distribution of the numbers of mutants in bacterial populations. J Genet 49:264–285

Lettier G et al (2006) The role of DNA double-strand breaks in spontaneous homologous recombination in *S. cerevisiae*. PLoS Genet 2:e194

Li WH, Gu Z, Wang H, Nekrutenko A (2001) Evolutionary analyses of the human genome. Nature 409:847–849

Lin FL, Sperle K, Sternberg N (1990) Intermolecular recombination between DNAs introduced into mouse L cells is mediated by a nonconservative pathway that leads to crossover products. Mol Cell Biol 10:103–112

Lindholm C, Edwards A (2004) Long-term persistence of translocations in stable lymphocytes from victims of a radiological accident. Int J Radiat Biol 80:559–566

Lloyd JA, McGrew DA, Knight KL (2005) Identification of residues important for DNA binding in the full-length human Rad52 protein. J Mol Biol 345:239–249

Lyndaker AM, Alani E (2009) A tale of tails: insights into the coordination of 3′ end processing during homologous recombination. Bioessays 31:315–321

Maines S, Negritto MC, Wu X, Manthey GM, Bailis AM (1998) Novel mutations in the RAD3 and SSL1 genes perturb genome stability by stimulating recombination between short repeats in *Saccharomyces cerevisiae*. Genetics 150:963–976

Manthey GM, Naik N, Bailis AM (2009) Msh2 blocks an alternative mechanism for non-homologous tail removal during single-strand annealing in *Saccharomyces cerevisiae*. PLoS One 4:e7488

Meltzer PS, Kallioniemi A, Trent JM (2002) Chromosomal alterations in human solid tumors. In: Vogelstein B, Kinzler KW (eds) The genetic basis of human cancer, 2nd edn. McGraw Hill, New York, pp 92–111

Meyer DH, Bailis AM (2008) Telomerase deficiency affects the formation of chromosomal translocations by homologous recombination in *Saccharomyces cerevisiae*. PLoS ONE 3:e3318

Mortensen UH, Bendixen C, Sunjevaric I, Rothstein R (1996) DNA strand annealing is promoted by the yeast Rad52 protein. Proc Natl Acad Sci USA 93:10729–10734

Mortensen UH, Erdeniz N, Feng Q, Rothstein R (2002) A molecular genetic dissection of the evolutionarily conserved N terminus of yeast Rad52. Genetics 161:549–562

Muller I et al (2005) Time-course of radiation-induced chromosomal aberrations in tumor patients after radiotherapy. Int J Radiat Oncol Biol Phys 63:1214–1220

Myers AM, Tzagoloff A, Kinney DM, Lusty CJ (1986) Yeast shuttle and integrative vectors with multiple cloning sites suitable for construction of lacZ fusions. Gene 45:299–310

Pannunzio NR, Manthey GM, Bailis AM (2008) RAD59 is required for efficient repair of simultaneous double-strand breaks resulting in translocations in *Saccharomyces cerevisiae*. DNA Repair (Amst) 7:788–800

Petukhova G, Stratton SA, Sung P (1999) Single strand DNA binding and annealing activities in the yeast recombination factor Rad59. J Biol Chem 274:33839–33842

Ray BL, White CI, Haber JE (1991) Heteroduplex formation and mismatch repair of the "stuck" mutation during mating-type switching in *Saccharomyces cerevisiae*. Mol Cell Biol 11:5372–5380

Reenan RA, Kolodner RD (1992) Characterization of insertion mutations in the *Saccharomyces cerevisiae* MSH1 and MSH2 genes: evidence for separate mitochondrial and nuclear functions. Genetics 132:975–985

Resnick MA, Martin P (1976) The repair of double-strand breaks in the nuclear DNA of *Saccharomyces cerevisiae* and its genetic control. Mol Gen Genet 143:119–129

Richardson C, Jasin M (2000) Frequent chromosomal translocations induced by DNA double-strand breaks. Nature 405:697–700

Ronne H, Rothstein R (1988) Mitotic sectored colonies: evidence of heteroduplex DNA formation during direct repeat recombination. Proc Natl Acad Sci USA 85:2696–2700

Sambrook J, Russell DW (2001) Molecular cloning: a laboratory manual. Cold Spring Harbor Laboratory Press, Cold Spring Harbor

Saparbaev M, Prakash L, Prakash S (1996) Requirement of mismatch repair genes MSH2 and MSH3 in the RAD1–RAD10 pathway of mitotic recombination in *Saccharomyces cerevisiae*. Genetics 142:727–736

Schiestl RH, Prakash S (1988) RAD1, an excision repair gene of *Saccharomyces cerevisiae*, is also involved in recombination. Mol Cell Biol 8:3619–3626

Schiestl RH, Igarashi S, Hastings PJ (1988) Analysis of the mechanism for reversion of a disrupted gene. Genetics 119:237–247

Schild D (1983) A note on the use of serial measures in spike train analysis and their relation to the corresponding moments. Int J Neurosci 18:247–252

Sherman F, Fink G, Hicks J (1986) Methods in yeast genetics. Cold Spring Harbor Laboratory Press, Cold Spring Harbor

Strout MP, Marcucci G, Bloomfield CD, Caligiuri MA (1998) The partial tandem duplication of ALL1 (MLL) is consistently generated by Alu-mediated homologous recombination in acute myeloid leukemia. Proc Natl Acad Sci USA 95:2390–2395

Sugawara N, Ira G, Haber JE (2000) DNA length dependence of the single-strand annealing pathway and the role of *Saccharomyces cerevisiae* RAD59 in double-strand break repair. Mol Cell Biol 20:5300–5309

Sung P (1997) Function of yeast Rad52 protein as a mediator between replication protein A and the Rad51 recombinase. J Biol Chem 272:28194–28197

Sung P, Reynolds P, Prakash L, Prakash S (1993) Purification and characterization of the *Saccharomyces cerevisiae* RAD1/RAD10 endonuclease. J Biol Chem 268:26391–26399

Thomas BJ, Rothstein R (1989) The genetic control of direct-repeat recombination in Saccharomyces: the effect of rad52 and rad1 on mitotic recombination at GAL10, a transcriptionally regulated gene. Genetics 123:725–738

Tomkinson AE, Bardwell AJ, Bardwell L, Tappe NJ, Friedberg EC (1993) Yeast DNA repair and recombination proteins Rad1 and Rad10 constitute a single-stranded-DNA endonuclease. Nature 362:860–862

Weinstock DM, Richardson CA, Elliott B, Jasin M (2006) Modeling oncogenic translocations: distinct roles for double-strand break repair pathways in translocation formation in mammalian cells. DNA Repair (Amst) 5:1065–1074

Wu Y, Sugiyama T, Kowalczykowski SC (2006) DNA annealing mediated by Rad52 and Rad59 proteins. J Biol Chem 281:15441–15449

Zhang F, Gu W, Hurles ME, Lupski JR (2009) Copy number variation in human health, disease, and evolution. Annu Rev Genomics Hum Genet 10:451–481